Technical Notes

TECHNICAL NOTES are short manuscripts describing new developments or important results of a preliminary nature. These Notes cannot exceed 6 manuscript pages and 3 figures; a page of text may be substituted for a figure and vice versa. After informal review by the editors, they may be published within a few months of the date of receipt. Style requirements are the same as for regular contributions (see inside back cover).

Thickness and Camber Effects in Slender Wing Theory

A. Plotkin*
University of Maryland, College Park, Maryland

Introduction

THE flow past thin slender wings with round leading edges can remain attached up to moderate values of angle of attack. For this reason, in the low aspect ratio limit, the slender wing theory of Jones[1] can provide a simple analytical tool to study this flow. It is the purpose of this Note to develop first-order corrections to slender wing theory due to spanwise thickness and camber.

For wings of general planform, the validity and applicability of slender wing theory have been extended recently with the addition of chordwise and compressibility corrections by Levin and Seginer.[2] Presumably, similar corrections could be applied to the present results.

Analysis

Consider the inviscid incompressible irrotational flow of a uniform stream of speed U at angle of attack α past a thin slender wing as shown in Fig. 1. The wing lies everywhere close to the x-y plane and is symmetric with respect to the x axis. The span increases in the stream direction and the trailing edge is straight. The wing surface is described by

$$F(x,y,z)=z-\epsilon f(x,y)=0 \qquad \epsilon \ll 1 \tag{1}$$

where ϵ is a small thickness or camber parameter. The root chord, maximum span, and aspect ratio are c, b, and A, respectively, and $A \ll 1$.

Wang[3] has used slender body theory and the method of matched asymptotic expansions to develop a "not-so-slender" wing theory as an expansion in aspect ratio. In general, for a slender body or wing, the near-field perturbation velocity potential has the form

$$\Phi=\phi+0(A^2, A^2 \log A) \tag{2}$$

For a wing of zero thickness and camber, ϕ is the slender wing solution of Jones[1] for the flow in the crossflow plane. An additional expansion in ϵ will be developed for ϕ. (Slender thin-body theory for wings at zero incidence is discussed in Weber.[4]) Unless $\epsilon \gg A^2 \log A$, the higher order terms (in A) in Eq. (2) must be retained and they are given (for $\epsilon=0$) in Wang.[3]

The mathematical problem for the near-field perturbation velocity potential (in the crossflow plane) is

$$\phi_{yy}+\phi_{zz}=0 \tag{3a}$$

$$\phi_z-\epsilon f_y \phi_y=0 \quad \text{on} \quad F=0 \tag{3b}$$

$$\phi(x,y,|z|\to\infty)=U\alpha z \tag{3c}$$

and the Kutta condition cannot be applied.

Consider the following thin wing expansion about the Jones[1] solution ϕ_0:

$$\phi=\phi_0+\epsilon\phi_1+\ldots \tag{4}$$

This expansion is substituted into Eqs. (3) and after a transfer of the wing boundary condition to $z=0$ and the use of the differential equation for ϕ_0, the problem for ϕ_1 becomes

$$\phi_{1_{yy}}+\phi_{1_{zz}}=0 \tag{5a}$$

$$\phi_{1_z}(x,y,0)=\frac{\partial}{\partial y}\left[f\phi_{0_y}(x,y,0)\right] \tag{5b}$$

$$\phi_{1_z}(x,y,|z|\to\infty)=0 \tag{5c}$$

The Jones[1] solution represents flow normal to a flat plate whose width is the local span $2s$ and is

$$\phi_0=U\alpha I\left[(y+iz)^2-s^2\right]^{1/2} \tag{6}$$

where I is the imaginary part. On the wing surface,

$$\phi_0(x,y,0\pm)=\pm U\alpha(s^2-y^2)^{1/2} \tag{7a}$$

$$\phi_{0_y}(x,y,0\pm)=\mp U\alpha y(s^2-y^2)^{-1/2} \tag{7b}$$

Let us write the cross-sectional shape in terms of camber and thickness components:

$$f(x,y)=C(x,y)\pm T(x,y) \tag{8}$$

Thickness Problem

The thickness part of ϕ_1 satisfies Eqs. (5a) and (5c) and with the use of Eqs. (7b) and (8), Eq. (5b) becomes

$$\phi_{1_z}(x,y,0\pm)=-U\alpha\frac{\partial}{\partial y}\left[yT(s^2-y^2)^{-1/2}\right] \tag{9}$$

This is identical to the camber problem of thin airfoil theory[5] without a Kutta condition. It can be solved by a distribution of vortices with strength $\gamma(y)$ per unit length and zero total circulation. ϕ_1 is

$$\phi_1=-\frac{1}{2\pi}\int_{-s}^{s}\gamma(\eta)\tan^{-1}\frac{y-\eta}{z}\,d\eta \tag{10}$$

and an application of Eq. (9) leads to

$$\gamma(y)=-\frac{2U\alpha}{\pi}(s^2-y^2)^{-1/2}\int_{-s}^{s}\frac{\partial}{\partial\eta}\left\{\eta T(x,\eta)(s^2-\eta^2)^{-1/2}\right\} \times\frac{(s^2-\eta^2)^{1/2}}{\eta-y}\,d\eta \tag{11}$$

Received Dec. 3, 1982; revision submitted Feb. 21, 1983.

*Professor, Department of Aerospace Engineering. Associate Fellow AIAA.

Also,

$$\phi_{l_y}(x,y,0\pm) = \pm\gamma(y)/2 \tag{12}$$

Camber Problem

The camber part of ϕ_l satisfies Eqs. (5a) and (5c) and with the use of Eqs. (7b) and (8), Eq. (5b) becomes

$$\phi_{l_z}(x,y,0\pm) = \mp U\alpha\frac{\partial}{\partial y}[yC(s^2-y^2)^{-1/2}] \tag{13}$$

This is identical to the thickness problem of thin airfoil theory[5] and can be solved by a source distribution to yield

$$\phi_l = -\frac{U\alpha}{2\pi}\int_{-s}^{s}\frac{\partial}{\partial\eta}\{\eta C(x,\eta)(s^2-\eta^2)^{-1/2}\}\ln[(y-\eta)^2+z^2]\mathrm{d}\eta \tag{14}$$

and on the wing surface

$$\phi_{l_y}(x,y,0\pm) = -\frac{U\alpha}{\pi}\int_{-s}^{s}\frac{\partial}{\partial\eta}\{\eta C(x,\eta)(s^2-\eta^2)^{-1/2}\}\frac{\mathrm{d}\eta}{y-\eta} \tag{15}$$

Results and Discussion

Consider a thin slender wing with an elliptic thickness distribution

$$T = (s^2-y^2)^{1/2} \tag{16}$$

With the use of Eqs. (11) and (12), we get

$$\phi_{l_y}(x,y,0\pm) = \mp U\alpha y(s^2-y^2)^{-1/2} \tag{17}$$

Consider a parabolic camber distribution

$$C = s(1-y^2/s^2) \tag{18}$$

With the use of Eq. (15), we get

$$\phi_{l_y}(x,y,0\pm) = -2U\alpha y/s \tag{19}$$

The linearized pressure relationship is

$$p = p_\infty - \rho U\phi_x \tag{20}$$

where p_∞ is the pressure in the stream and ρ is the density. The pressure jump across the wing (cross-sectional lift) is

$$\Delta L = p(x,y,0-) - p(x,y,0+)$$

$$= \rho U\frac{\partial}{\partial x}[\phi(x,y,0+) - \phi(x,y,0-)] \tag{21}$$

It is noted that, to first order in ϵ, thickness contributes lift but camber does not. Camber enters lift at the next order in aspect ratio.

The lift is obtained by an integration of the pressure jump over the wing surface, and, after a chordwise integration, it becomes

$$L = \rho U\int_{-s}^{s}[\phi(c,y,0+) - \phi(c,y,0-)]\mathrm{d}y \tag{22}$$

For the Jones[1] basic slender wing theory, use of ϕ_0 from Eqs. (7) yields

$$C_L \equiv 2L/\rho U^2 S = \pi A\alpha/2 \tag{23}$$

where S is the planform area. For a wing with an elliptical cross section, a comparison between Eqs. (17) and (7b) shows that the total lift coefficient should be

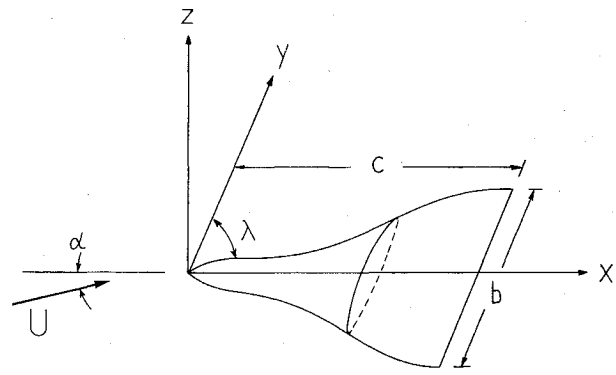

Fig. 1a Configuration and coordinate system.

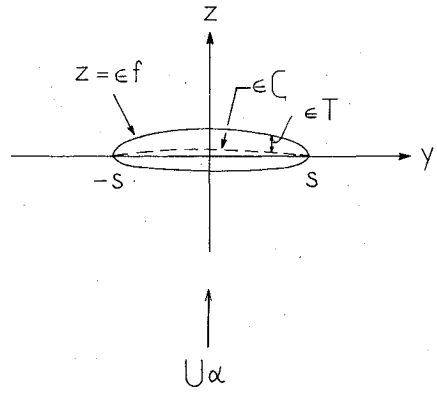

Fig. 1b Cross-flow plane geometry.

$$C_L = \pi A\alpha(1+\epsilon)/2 \tag{24}$$

It is noted that for the elliptic thickness distribution, for small angles of attack when the flow is attached, the lift increases with increasing thickness. Kulfan[6] shows that the vortex lift decreases with thickness as the angle of attack increases and the flow separates from the leading edge.

Let us now consider a thin slender wing with elliptical cross section and no camber. The surface is given by

$$z = \pm\epsilon(s^2-y^2)^{1/2} \tag{25}$$

where ϵ is the thickness ratio of the cross section. On the wing surface, the perturbation velocity potential is

$$\phi(x,y,0\pm) = \pm U\alpha(1+\epsilon)(s^2-y^2)^{1/2} \tag{26}$$

The slender wing surface speed is given by

$$(Q/U)_{sw} = 1 + (\phi_x/U) = 1 \pm \alpha s s'(1+\epsilon)(s^2-y^2)^{-1/2} \tag{27}$$

and it is seen to exhibit the leading edge square-root singularity that is characteristic of slender wing theory.

A leading-edge correction can be applied to render the solution valid in the neighborhood of the round leading edge. Van Dyke[7] states that the local leading-edge flow is the flow past a semi-infinite parabola whose nose radius is the radius of curvature of the section perpendicular to the leading edge. If this nose radius is denoted by $r(x)$, the surface speed with correction included is

$$\frac{Q}{U} = \left(\frac{Q}{U}\right)_{sw}\left[\frac{y+s}{y+s+r\sin\lambda/2}\right]^{1/2} \qquad y<0 \tag{28}$$

where $\lambda(x)$ is the sweep angle. For the elliptic section, the nose radius in the crossflow plane is $s\epsilon^2$. The nose radius in Eq. (28) is then $r = s\sin\lambda\epsilon^2$.

The wing surface pressure distribution with leading-edge correction included is

$$C_p = 1 - Q^2/U^2 \tag{29}$$

where Q/U is given in Eq. (28).

Acknowledgments

This research was supported by NASA Langley Research Center under Grant NCC1-41. The author wishes to thank Dr. John Lamar of NASA for his help and interest throughout the course of the research.

References

[1] Jones, R. T., "Properties of Low-Aspect-Ratio Pointed Wings at Speeds Below and Above the Speed of Sound," NACA Rept. 835, 1946.

[2] Levin, D. and Seginer, A., "Chordwise and Compressibility Correction for Arbitrary Planform Slender Wings," *AIAA Journal*, Vol. 20, Aug. 1982, pp. 1025-1030.

[3] Wang, K. C., "A New Approach to 'Not-so-Slender' Wing Theory," *Journal of Mathematics and Physics*, Vol. XLVII, No. 4, Dec. 1968, pp. 391-406.

[4] Weber, J., "The Calculation of the Pressure Distribution on Thick Wings of Small Aspect Ratio at Zero Lift in Subsonic Flow," Aeronautical Research Council, R&M 2993, Sept. 1954.

[5] Cheng, H. K. and Rott, N., "Generalizations of the Inversion Formula of Thin Airfoil Theory," *Journal of Rational Mechanics and Analysis*, Vol. 3, No. 3, May 1954, pp. 357-382.

[6] Kulfan, R. M., "Wing Airfoil Shape Effects on the Development of Leading-Edge Vortices," AIAA Paper 79-1675, 1979.

[7] Van Dyke, M. D., "Subsonic Edges in Thin-Wing and Slender-Body Theory," NACA TN 3343, 1954.

Cellular Patterns in Poststall Flow over Unswept Wings

D. Weihs* and J. Katz†
Technion – Israel Institute of Technology
Haifa, Israel

Introduction

THE growing fleet of general aviation aircraft has focused increased attention on the poststall aerodynamics of unswept wings, with the purpose of improving the stall/spin resistant characteristics of these airplanes. Flow visualization experiments[1-7] with such wings indicated that beyond stall the nature of the separated flow is strongly three-dimensional, even when very high-aspect-ratio wing planforms were tested. Under those conditions the oil flow patterns on the upper surface of the wings appeared to be cellular in shape, similar to the one shown in Fig. 1. Furthermore, it was observed that when the wing aspect ratio is increased the number of cells grows, with limited variation in the "natural size" of these cells.[6]

No theoretical interpretation exists for the prediction of the nature of this complex three-dimensional flow. Therefore, this Note proposes a mechanism for the production of such cells based on an analysis of the stability of the separation vortices. This enables an approximate calculation of the large-scale geometry of the separation cells.

Received June 24, 1982; revision received Nov. 30, 1982.

*Professor, Department of Aeronautical Engineering.

†Senior Lecturer, Department of Mechanical Engineering. Member AIAA.

The Flow Model

As a result of increasing the angle of attack of the high-aspect-ratio unswept wing up to the fully stalled flow condition, a separation line will initially progress forward on the wing upper surface. The location of this line will be prescribed by the wing camber, angle of attack, and Reynolds number. Along this separation line a shear flow regime exists that constantly generates vorticity, as shown in Fig. 2a. This vorticity is aggregated to form a "time average/vortex core" that pulsates both in location and strength to generate the well-known von Kármán street vortex pattern observed in the two-dimensional cross section.[8-10] However, the pure two-dimensional (or straight) vortex core of Fig. 2a is not stable and a wavy disturbance will develop (Fig. 2b), resulting in the three-dimensional time-averaged vortex pattern proposed in Fig. 2c. Surface oil flow visualization conforming to this model will result in formations as shown by Fig. 2d, which are similar to those reported in many experiments (Refs. 1-7 and Fig. 1).

To study the production of the cellular spanwise structure of the separated wake, we return to the case of Fig. 2a and specifically to the vortex above the upper surface of the wing (Fig. 3). As mentioned above, it is assumed that the configuration of Fig. 2a is the time-averaged configuration, with further vorticity buildup being periodically shed into the wake. Thus, we have the quasi-two-dimensional situation of Fig. 3 where the vortex core is located such that the relative velocity between point "a" and the wing is zero. The profile serves approximately as a reflecting plane for the vortex, i.e., resulting in an equivalent image vortex. Assuming the upper surface of the wing to be approximately flat in the region

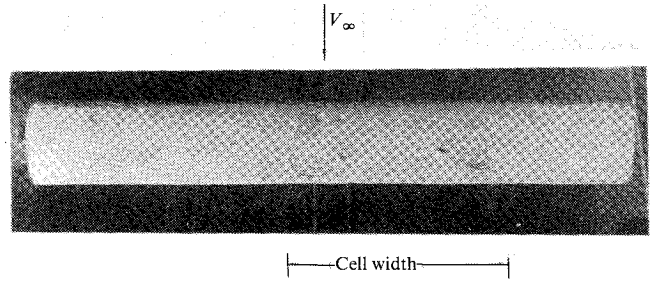

Fig. 1 Oil flow patterns on the upper surface of a stalled wing (NACA 0012 airfoil at $\alpha = 14$ deg, $\mathcal{R} = 7$, $Re = 0.2 \times 10^5$).

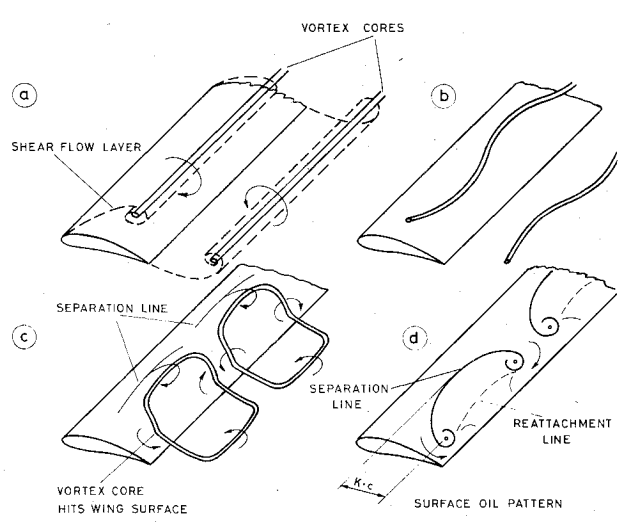

Fig. 2 Schematic of the vortex instability and the resulting cellular shapes in the separated flow over rectangular wings.